



# Characteristics of geochemistry and benthic communities in microbial mat-covered sediments related to methane seepage, northeastern Japan Sea

Yuki Ota, Masahiro Suzumura, Ayumi Tsukasaki, Atsushi Suzuki, Akira Iguchi, Miyuki Nishijima, Hideyoshi Yoshioka, Tomo Aoyagi, Tomoyuki Hori  
(National Institute of Advanced Industrial Science and Technology)



## INTRODUCTION

A depression on top of Sakata Knoll, the northeastern Japan Sea, corresponds to a gas-hydrate-bearing area with seepage of methane-rich fluid, and microbial mats patchily cover the seafloor sediments (Fig. 1). We investigated characteristics of benthic macrofaunal communities and geochemical parameters in and around microbial mat-covered sediments on the knoll.

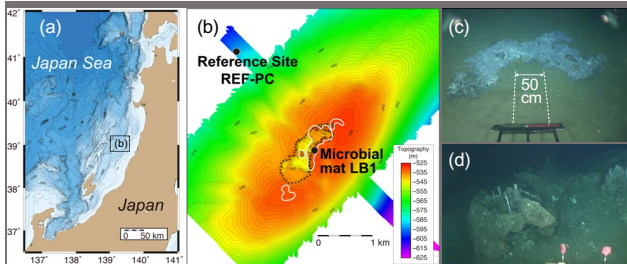


Fig. 1 Bathymetric maps of the study area showing the eastern margin of the Japan Sea with 100-m depth contours (a), and Sakata Knoll with 0.5-m contours (b). A depression on top of the knoll and areas where patchy microbial mats were found are outlined with black dashed and white lines, respectively, in (b). And, photographs of the studied sediments covered by microbial mat LB1 (c) and the surrounding carbonate clusters (d). White dashed lines in (c) traced the ROV beamlines.

## METHOD

Sediment cores were collected at three sites for this study: one within a microbial mat, a second a few meters outside of the microbial mat, and a third from a reference site outside the gas-hydrate-bearing areas (Fig. 2). For these cores, the interstitial sulfate ( $SO_4^{2-}$ ) and sulfide ( $H_2S$ ) ion concentrations, sedimentary total sulfur (TS), and trace-element contents, carbon stable isotopic compositions of sediment bulk carbonate minerals ( $\delta^{13}C_{TIC}$ ), and 18S rRNA gene sequencing were analyzed. Details of the method are presented in Ota et al (2022, 2024). The enrichment factor (EF) was calculated to assess the enrichment levels of elements in these sediments as follows:

$$EF_X = (X/AI)_{\text{sample}} / (X/AI)_{\text{background}}$$

where  $(X/AI)_{\text{sample}}$  is the ratio of the trace element X content to the aluminum content in the sediment sample and  $(X/AI)_{\text{background}}$  is the ratio of the upper continental crust (McLennan, 2001). To determine the authigenic element enrichments excluding the influence of terrigenous element inputs, EF is normalized against the sediment AI. Values of  $EF > 25$  are defined as severe enrichment (Birth, 2003).

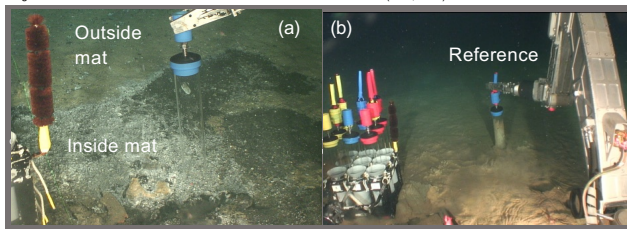
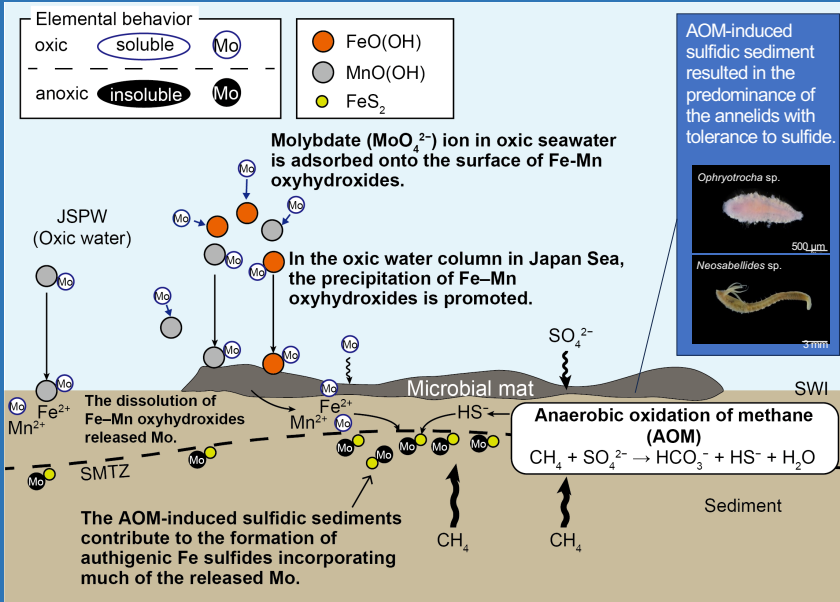


Fig. 2 Images showing the sampling of push cores in microbial mat LB1 (a) and the reference site (b). The outer diameter of core pipe is 7.6 cm.

## Conclusion:

The characteristics of benthic macrofaunal communities and geochemical parameters in and around microbial mat-covered sediments in Sakata Knoll may be associated with the sulfidic sediment formed by AOM and oxic environment in water column.



SWI: sediment-water interface, SMTZ: sulfate-methane transition zone, JSPW: Japan Sea Proper Water.

Details of studies presented in this poster show as follows:



Ota et al. 2022, Chem. Geol.



Ota et al. 2024, Chemosphere

Supplement data including Poster file:



## RESULTS & DISCUSSIONS

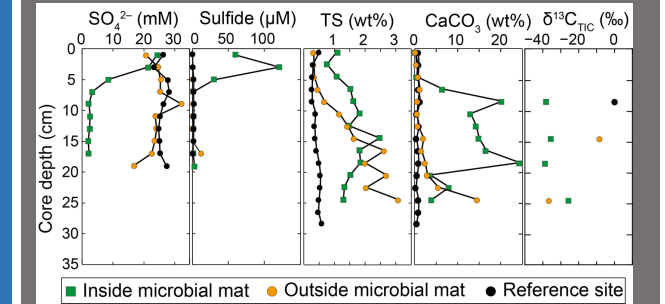


Fig. 3 Depth profiles geochemical parameters in sediments for sites inside and outside the microbial mat LB1, and at a reference site on Sakata Knoll.

Geochemical features (e.g., high TS contents and strong negative values of  $\delta^{13}C_{TIC}$  compared with these values at reference site) in the surface sediment inside the microbial mat indicated the occurrence of active anaerobic oxidation of methane (AOM) (Fig. 3).

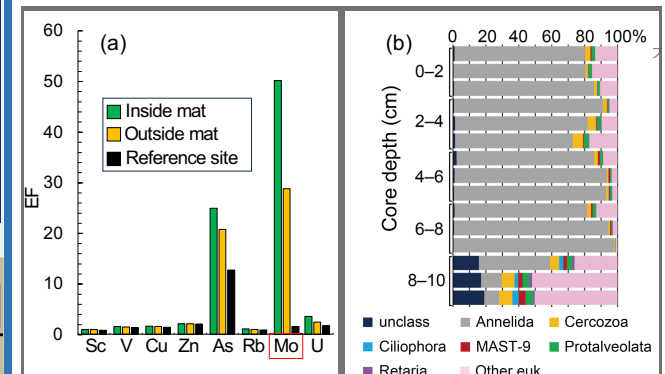


Fig. 4 (a) Average EF values in sediment cores for sites inside and outside the microbial mat LB1, and at a reference site on Sakata Knoll. (b) Relative read abundance of amplicon sequence variants annotated at the phylum level of eukaryotes from sites inside the microbial mat LB1.

The EF value for molybdenum (Mo) in cores collected in this study indicates strong enrichments of Mo in the sediment inside the mat, suggesting that the AOM-derived  $H_2S$  favored the capture of Mo on sulfide minerals (Fig. 4a). Because of the non-enrichments of other elements, Mo may be efficiently transported into the AOM-induced sulfidic seafloor by adsorption on the particulate Fe-Mn hydroxides that are well preserved in oxic water column of the Japan Sea Proper Water (Fig. S2 in supplement file).

Both the 18S rRNA genes (Fig. 4b) and morphological analyses showed that the sediment inside the microbial mat noticeably favored annelids, with dorvilleid *Ophryotrocha* sp. and ampharetid *Neosabellides* sp. identified as major constituents. The AOM-induced sulfidic sediment conditions resulted in the predominance of these annelids with tolerance to sulfide.

Supporting Material for:

**Characteristics of geochemistry and benthic communities in microbial mat-covered sediments  
related to methane seepage, northeastern Japan Sea**

Yuki Ota<sup>a\*</sup>, Masahiro Suzumura<sup>a</sup>, Ayumi Tsukasaka<sup>a</sup>, Atsushi Suzuki<sup>b,c</sup>, Akira Iguchi<sup>b,c</sup>, Miyuki  
Nishijima<sup>b</sup>, Hideyoshi Yoshioka<sup>b</sup>, Tomo Aoyagi<sup>a</sup>, Tomoyuki Hori<sup>a</sup>

<sup>a</sup> Department of Energy and Environment, National Institute of Advanced Industrial Science and  
Technology (AIST), Onogawa 16-1, Tsukuba, Ibaraki 305-8561, Japan

<sup>b</sup> Geological Survey of Japan, National Institute of Advanced Industrial Science and Technology  
(AIST), Higashi 1-1-1, Tsukuba, Ibaraki 305-8567, Japan

<sup>c</sup>Research Laboratory on Environmentally-Conscious Developments and Technologies [E-code],  
National Institute of Advanced Industrial Science and Technology (AIST), Tsukuba 305-8567, Japan

## Study area

The Japan Sea is a semi-enclosed marginal sea in the northwestern Pacific with a maximum depth of about 3800 m. Winter cooling causes saline surface water in the northwestern part of the Japan Sea to sink, forming homogeneous cold, saline, and well-oxygenated deep and bottom water below about 300 m, known as Japan Sea Proper Water (Senjyu et al., 2005; Gamo et al., 2014). This water has a temperature of 0–1 °C, a salinity of 34.1, and a high concentration of dissolved oxygen ( $>200 \mu\text{mol kg}^{-1}$ ) (Senjyu et al., 2013; Gamo et al., 2014).

More than a decade of scientific exploration has revealed the occurrence and formation of methane hydrate in several areas of the eastern margin of the Japan Sea (e.g., Matsumoto et al., 2011; Yanagawa et al., 2014; Hiruta et al., 2014; Goto et al., 2017). Sakata Knoll (approx. 15 km long  $\times$  5–10 km wide, and measuring about 120 m in height relative to the southwestern foot of the knoll) is part of a potential area of massive shallow methane hydrates in the eastern margin of the Japan Sea (Fig. S1). In this area, gas chimney structures formed by the upward migration of methane gas that accumulates as gas hydrates have been identified as zones of acoustic blanking on sub-bottom profile images (Asda et al., 2022; Matsumoto et al., 2017). The top of the knoll has a depression approximately 1 km  $\times$  300–400 m in extent and about 12 m deep, bordered by steep slopes. The depression contains two terraces, in the northern and southern parts, and a single hill near the center.

The studied area of the seafloor in the depression on Sakata Knoll (50,800 m<sup>2</sup>) was mainly covered by pelagic sediment, but patchily distributed microbial mats and carbonates were also present (Asada et al., 2022; Miyajima et al., 2023, 2024; Ota et al., 2022, 2024). The microbial mats were relatively large and dense along the hills and small ridges in the center, and on the southwestern slope of the depression. Some mats were also detected on the northern and southern terraces within the depression. The observed microbial mats appeared to be less than 1 cm thick. Most of the

observed microbial mats were less than 1 m in diameter, but some were 4–5 m in diameter. In total, approximately 350 microbial mats were observed. More details of the study area are presented elsewhere (Ota et al., 2022).

## **Materials and methods**

### *Sampling*

Sediment samples were collected at Sakata Knoll during expedition SS20-1, 6–23 July 2020, using ROV *Hakuyo 3000* of the towing and salvage vessel *Shinsei-maru* (Fukada Salvage Co. Ltd., Osaka, Japan). The undisturbed surface-sediment samples were collected during the campaign using a MBARI polycarbonate push core (40-cm length, 7-cm inner diameter, 6-mm wall thickness). Push-core samples were taken at two sites within the depression on top of the knoll (a gas hydrate-bearing area)—one inside (LB1-PC-IBM, water depth 542 m) and one outside (LB1-PC-OBM, water depth 541 m) microbial mat LB1—and at a reference site approximately 2 km northwest of the depression (REF-PC: 39°01'N, 139°17'E, water depth 596 m) (Fig. 1). On the basis of the investigation of acoustic velocity anomalies, the reference site was regarded as an area without methane hydrates or methane seepage at the seafloor or the shallow subseafloor approximately 50 m below the seafloor (Asada et al., 2022). The sites LB1-PC-IBM and LB1-PC-OBM were only about 5 meters apart. Three push cores were obtained at each site, which were used for interstitial water sampling, DNA meta-barcoding analysis, and geochemical measurements, respectively.

Interstitial water samples were collected by using a pressurized core interstitial-water sampler and Rhizon samplers to avoid exposing the interstitial water samples to air. Details of the method for collecting interstitial water samples from the sediment cores are presented elsewhere (Ota et al., 2022). Immediately after extraction, the interstitial water samples were filtered through a 0.2- $\mu$ m

syringe filter. For the measurement of dissolved hydrogen sulfide in interstitial water, 1-mL aliquots of interstitial water were transferred to 1.5-mL tubes containing 40  $\mu$ L of 2 N zinc acetate solution to preserve dissolved sulfide as zinc sulfide. These samples were stored at 4°C on board. Recovered push core samples for DNA meta-barcoding analysis were immediately extruded on board and sectioned into 2 cm lengths. Sediment sections were transferred into Petri dishes, and these dishes were packed in plastic vacuum bags using a vacuum sealer to avoid the oxidation of the sediment samples and stored at –80°C on board. Push core samples for geochemical measurements were immediately closed with rubber stoppers without draining water overlying the sediments in order to avoid sediment oxidation during transportation and preservation and stored at 4°C on board. Subsequently, in the onshore laboratory, these sediment cores were longitudinally split into two sections using fishing line, photographed, and subsampled at 1-cm intervals. Analytical procedures of geochemical analyses and 18S rRNA gene sequencing are presented elsewhere (Ota et al., 2022, 2024).

#### *Physical and chemical properties of the water column*

Water-column profiles of temperature, salinity, and dissolved oxygen concentrations were measured using a conductivity–temperature–depth (CTD) carousel multisampler system equipped with a dissolved oxygen sensor SBE-43 (Sea Bird Electronics, Inc.) at stations CTD1 above northwestern Sakata Knoll (39°1.830' N, 139°16.200' E, water depth 681 m) and CTD3 (38°59.822' N, 139°18.221' E, water depth 539 m) (Fig. S1).

## Results

### *CTD observation and chemical analyses of seawater*

The physical structure and composition of the water columns in and around Sakata Knoll were very similar (Fig. S2). The temperatures of the water column over the knoll ranged from ~21.6°C in the surface water to ~0.5°C in the deepest water (~680 m). The salinity ranged between ~33.7 and ~34.3. The dissolved oxygen concentrations remained almost constant and high, with small fluctuations, with values between 288.4  $\mu\text{mol/L}$  at ~30–50 m and 189.5  $\mu\text{mol/L}$  in the deepest water (~680 m). The dissolved oxygen concentrations in bottom water measured by ROV were also high at core sites LB1 (196.9  $\mu\text{mol/L}$ ) and REF-PC (203.1  $\mu\text{mol/L}$ ) (Fig. S2).

Details of the results of other analyses including the trace element compositions in the interstitial water (Fig. S3) and the solid-phase of sediments (Fig. S4 and Table S1) are presented elsewhere (Ota et al., 2022).

**Fig. 1.** Bathymetric maps of the study area showing (a) the eastern margin of the Japan Sea with 100-m depth contours, (b) the location of Sakata Knoll with 100-m depth contours, and (c) the main study site with the locations of sampling sites on Sakata Knoll with 0.5-m contours, modified from Ota et al. (2022). White circles in (b) and (c) are conductivity–temperature–depth (CTD) measurement sites and black circles are sediment core locations.

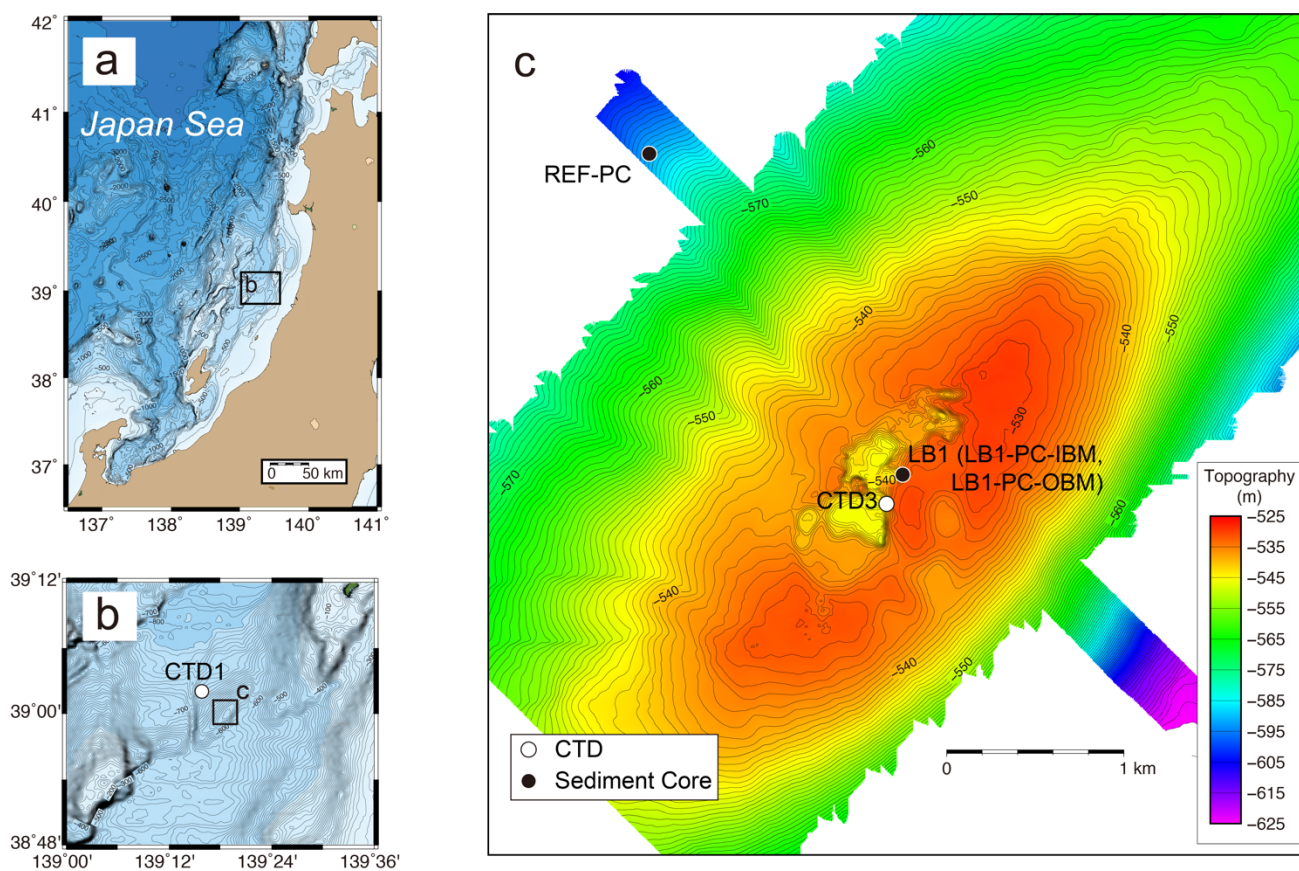


**Fig. S2.** Vertical profiles of (a) temperature, (b) salinity, and (c) dissolved oxygen concentrations and (d) the temperature–salinity (T–S) diagram for all depths at stations CTD1 (black line) and CTD3 (red line) at Sakata Knoll, modified from Ota et al. (2022). Part (c) also shows the dissolved oxygen concentrations of bottom water collected from the sampling sites of cores LB1-PC-IBM and REF-PC. The gray lines in (d) represent the potential density anomaly ( $\text{kg/m}^3$ ).

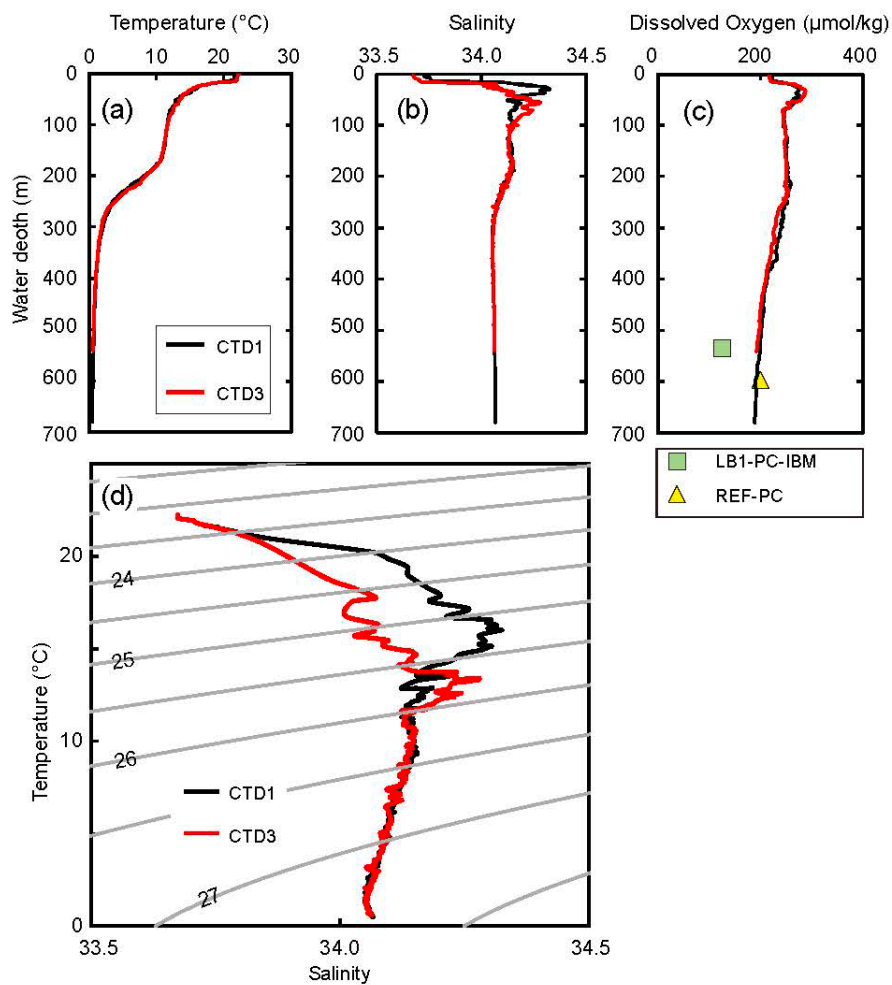




**Fig. S4.** Depth profiles of the levels and enrichment factors (EF) of molybdenum within sediment cores from Sakata Knoll, modified from Ota et al. (2022).

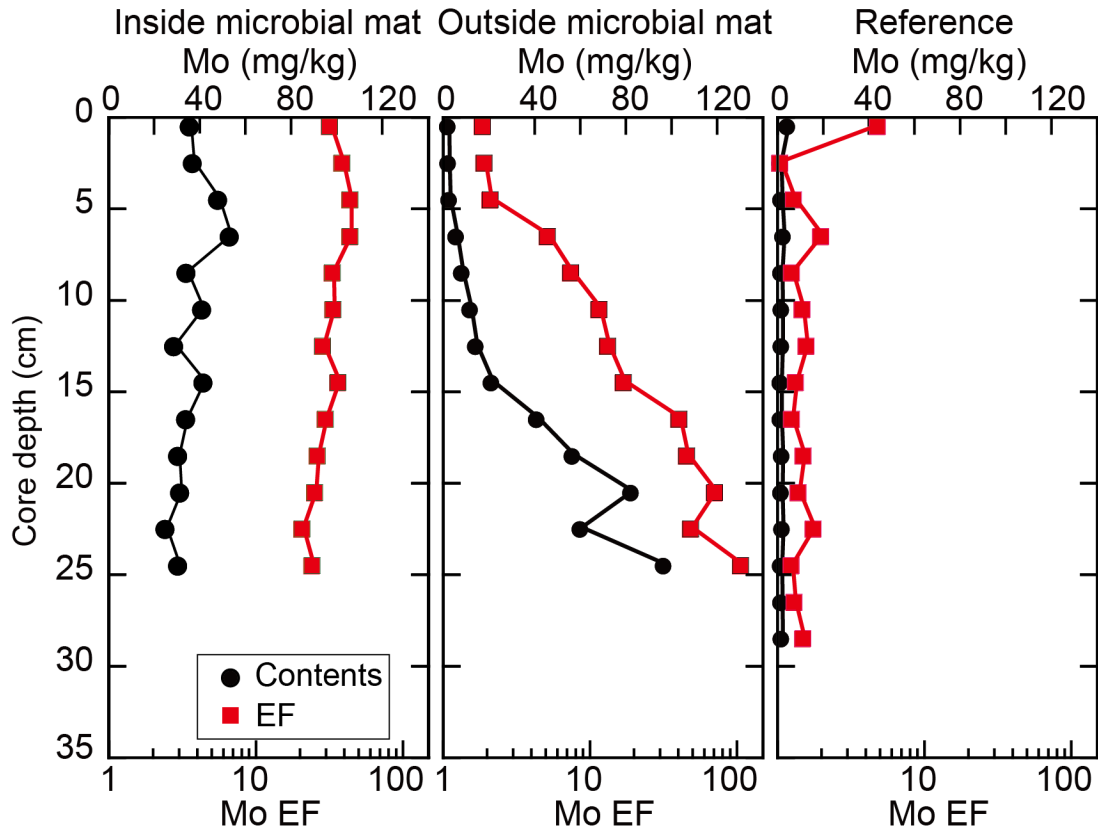


Table S1. Enrichment factors of trace elements in Sakana Knoll sediment cores collected inside (LBI-PC-IBM) and outside the microbial mat LBI (LBI-PC-OBM), and at the reference site (REF-PC), modified from Ota et al. (2022).

Core	Depth (cm)	Sc	V	Mn	Fe	Cu	Zn	As	Rb	Mo	La	Ce	Pr	Nd	Sm	Eu	Gd	Tb	Dy	Ho	Tm	Yb	Lu	Pb	Th	U		
LBI-PC-IBM	0.5	0.88	1.41	0.76	1.09	1.36	1.83	12.15	0.87	31.76	1.05	1.07	1.09	1.16	1.32	2.79	1.72	1.39	1.52	1.31	1.37	1.30	1.38	1.37	0.38	0.94	1.85	
	2.5	0.96	1.54	0.79	1.19	1.49	1.94	11.73	0.93	38.56	0.90	0.89	0.98	1.09	1.39	2.59	1.73	1.48	1.51	1.29	1.38	1.34	1.41	1.35	0.42	0.97	1.77	
	4.5	0.92	1.55	0.79	1.22	1.62	1.98	12.02	0.96	43.74	0.85	0.89	0.90	1.00	1.22	1.63	1.51	1.29	1.35	1.18	1.21	1.24	1.27	1.28	0.45	0.93	1.73	
	6.5	0.94	1.47	0.78	1.17	1.52	1.84	12.32	0.91	43.73	0.89	0.89	0.92	0.99	1.15	1.52	1.51	1.21	1.29	1.12	1.18	1.12	1.24	1.21	0.39	0.93	2.51	
	8.5	0.92	1.44	0.78	1.20	1.40	1.74	18.71	0.90	33.07	0.98	0.99	1.00	1.12	1.44	1.65	1.66	1.40	1.54	1.33	1.33	1.33	1.39	1.38	0.27	0.94	5.57	
	10.5	0.90	1.46	0.75	1.17	1.45	1.83	15.90	0.92	33.54	0.96	0.95	0.99	1.07	1.33	1.56	1.68	1.39	1.43	1.25	1.31	1.24	1.27	1.30	0.32	0.96	3.69	
	12.5	0.90	1.46	0.76	1.13	1.38	1.73	17.49	0.93	28.46	1.03	1.03	1.07	1.17	1.44	1.69	1.74	1.49	1.56	1.37	1.37	1.39	1.32	1.43	0.25	0.99	4.78	
	14.5	0.93	1.46	0.80	1.37	1.38	1.80	34.62	0.95	36.17	1.08	1.07	1.11	1.21	1.45	1.74	1.90	1.65	1.66	1.48	1.47	1.46	1.50	1.44	0.23	1.08	4.56	
	16.5	0.92	1.43	0.79	1.19	1.36	1.71	17.05	0.92	29.67	1.04	1.03	1.06	1.18	1.39	1.68	1.74	1.54	1.57	1.38	1.43	1.41	1.42	1.46	0.23	1.01	4.06	
	18.5	0.91	1.44	0.77	1.22	1.38	1.76	24.91	0.93	26.18	1.03	1.02	1.07	1.13	1.47	1.63	1.73	1.46	1.52	1.31	1.28	1.29	1.41	1.37	0.23	1.02	3.27	
	20.5	0.92	1.45	0.79	1.10	1.47	1.80	16.32	0.94	25.04	0.96	0.98	1.02	1.12	1.38	1.70	1.69	1.51	1.47	1.27	1.27	1.42	1.38	1.51	0.24	1.01	2.13	
	22.5	1.02	1.60	0.73	1.10	1.57	1.91	14.03	1.01	20.54	1.11	1.04	1.20	1.28	1.60	1.99	2.04	1.81	1.79	1.71	1.64	1.77	1.60	1.84	0.26	1.12	3.01	
	24.5	0.95	1.54	0.70	1.08	1.54	1.82	10.99	0.99	24.05	1.02	1.03	1.08	1.17	1.45	1.82	1.82	1.62	1.60	1.49	1.40	1.67	1.51	1.73	0.24	1.04	2.69	
	LBI-PC-OBM	0.5	0.83	1.46	0.76	1.15	1.56	2.09	7.33	0.98	1.90	0.93	0.97	0.98	1.04	1.31	1.80	1.61	1.56	1.47	1.40	1.29	1.68	1.39	1.65	0.49	1.00	1.39
		2.5	1.04	1.75	0.86	1.33	1.90	2.48	8.16	1.24	2.36	1.11	1.02	1.21	1.30	1.60	2.34	2.00	1.96	1.90	1.70	1.67	2.16	1.79	2.09	0.62	1.16	1.89
4.5		0.85	1.36	0.69	1.06	1.39	1.87	7.28	0.95	1.95	0.91	0.93	0.92	1.01	1.21	1.61	1.58	1.33	1.35	1.17	1.22	1.21	1.30	1.26	0.42	0.98	1.51	
6.5		0.90	1.60	0.74	1.24	1.64	2.14	10.66	1.12	5.77	1.00	1.00	1.04	1.13	1.41	1.85	1.79	1.51	1.49	1.34	1.41	1.42	1.53	1.44	0.45	1.07	2.13	
8.5		0.89	1.50	0.70	1.20	1.54	1.99	14.71	1.00	7.76	0.97	0.96	0.97	1.03	1.30	1.75	1.58	1.33	1.40	1.17	1.28	1.25	1.36	1.29	0.41	1.00	2.08	
10.5		0.86	1.41	0.72	1.19	1.42	1.84	25.76	0.95	10.88	0.96	1.00	0.98	1.06	1.29	1.57	1.54	1.34	1.40	1.19	1.20	1.23	1.27	1.26	0.36	1.02	1.84	
12.5		0.91	1.48	0.81	1.31	1.50	1.93	26.38	1.00	13.42	0.96	1.00	1.00	1.11	1.34	1.90	1.67	1.43	1.49	1.28	1.36	1.33	1.44	1.36	0.37	1.01	2.04	
14.5		0.92	1.42	0.91	1.30	1.45	1.85	22.93	0.96	16.55	0.91	0.93	0.94	1.03	1.28	1.63	1.64	1.36	1.42	1.22	1.25	1.22	1.24	1.29	0.34	0.98	2.00	
16.5		0.85	1.47	0.99	1.52	1.46	1.88	44.41	0.93	38.07	0.85	0.90	0.88	0.97	1.25	1.51	1.50	1.25	1.38	1.16	1.25	1.29	1.31	1.48	0.33	0.97	2.38	
18.5		0.79	1.64	0.93	1.31	1.56	1.88	17.48	0.93	43.50	0.88	0.95	0.94	1.04	1.31	1.53	1.60	1.39	1.48	1.25	1.33	1.31	1.43	1.48	0.27	0.98	2.96	
20.5		0.95	1.80	1.11	1.57	1.56	2.01	22.52	0.97	72.71	0.91	0.93	0.95	1.03	1.29	1.59	1.62	1.38	1.47	1.28	1.33	1.30	1.43	1.38	0.27	0.96	3.49	
22.5		0.96	1.62	0.96	1.25	1.48	1.82	15.36	0.91	46.00	0.92	0.90	0.97	1.07	1.35	1.51	1.62	1.36	1.50	1.31	1.39	1.33	1.37	1.46	0.25	0.94	3.57	
24.5		0.87	1.49	1.10	1.66	1.36	1.73	35.02	0.86	92.97	0.88	0.90	0.93	1.00	1.26	1.47	1.57	1.33	1.48	1.27	1.34	1.25	1.38	1.31	0.22	0.90	4.72	
0.5		0.79	1.58	0.81	1.48	1.77	3.33	19.61	0.92	5.13	0.81	0.72	0.86	0.96	1.19	1.57	1.48	1.33	1.37	1.24	1.24	1.21	1.35	1.41	0.66	0.93	0.78	
2.5		0.97	1.67	0.91	1.24	1.82	2.61	6.56	1.08	1.20	0.92	0.89	0.98	1.05	1.34	1.58	1.58	1.38	1.45	1.32	1.37	1.42	1.41	1.45	0.66	1.06	1.78	
4.5	0.89	1.60	0.85	1.25	1.73	2.44	6.82	1.02	1.41	0.95	0.97	0.98	1.08	1.30	1.64	1.60	1.36	1.42	1.28	1.37	1.25	1.37	1.42	0.60	1.04	1.84		
6.5	1.35	1.60	0.82	1.22	1.66	2.31	7.51	1.33	2.20	0.99	0.92	1.00	1.10	1.37	1.62	1.61	1.39	1.40	1.25	1.26	1.31	1.27	1.29	0.58	1.05	2.04		
8.5	0.82	1.47	0.76	1.17	1.60	2.12	9.83	0.98	1.31	0.89	0.95	0.91	0.98	1.16	1.46	1.47	1.23	1.30	1.12	1.21	1.18	1.27	1.30	0.47	1.00	2.01		
10.5	1.02	1.39	0.70	1.14	1.44	1.93	11.24	0.96	1.47	0.84	0.90	0.84	0.89	1.04	1.39	1.39	1.14	1.23	1.02	1.07	1.12	1.14	1.13	0.46	0.97	1.83		
12.5	0.80	1.30	0.72	1.12	1.37	1.88	10.14	0.95	1.44	0.91	0.98	0.92	1.00	1.20	1.44	1.47	1.23	1.27	1.11	1.19	1.21	1.24	1.24	0.38	0.99	1.82		
14.5	0.71	1.55	0.82	1.31	1.59	2.18	13.78	0.96	1.45	0.96	0.99	0.97	1.04	1.29	1.60	1.59	1.58	1.39	1.15	1.26	1.28	1.32	1.32	0.44	1.03	1.78		
16.5	0.71	1.55	0.84	1.32	1.65	2.16	12.64	0.95	1.38	0.95	1.02	0.97	1.07	1.32	1.63	1.62	1.34	1.41	1.22	1.27	1.23	1.33	1.27	0.45	1.01	2.05		
18.5	0.80	1.28	0.73	1.17	1.34	1.85	16.81	0.94	1.41	0.91	0.95	0.92	0.98	1.17	1.42	1.49	1.23	1.29	1.12	1.19	1.20	1.26	1.29	0.34	0.99	1.95		
20.5	0.81	1.33	0.74	1.15	1.37	1.90	17.43	0.89	1.34	0.89	0.93	0.92	0.99	1.16	1.48	1.47	1.21	1.27	1.12	1.23	1.17	1.23	1.21	0.34	0.97	2.11		
22.5	0.83	1.23	0.73	1.14	1.26	1.77	15.59	0.90	1.59	0.87	0.92	0.89	0.95	1.18	1.37	1.41	1.20	1.30	1.13	1.18	1.19	1.29	1.22	0.30	0.92	1.80		
24.5	0.84	1.24	0.75	1.10	1.29	1.80	16.12	0.89	1.16	0.85	0.90	0.87	0.97	1.17	1.49	1.47	1.23	1.29	1.18	1.17	1.24	1.21	1.31	0.31	0.94	1.79		
26.5	0.89	1.30	0.92	1.19	1.35	1.92	14.18	0.87	1.33	0.88	0.95	0.94	1.02	1.32	1.62	1.70	1.45	1.53	1.42	1.47	1.53	1.51	1.46	0.33	1.09	1.58		
28.3	0.76	1.03	0.57	0.93	1.03	1.42	12.97	0.73	1.12	0.70	0.78	0.71	0.76	0.95	1.07	1.15	0.97	0.99	0.89	0.92	0.92	0.97	0.97	0.24	0.81	1.58		

## References

- Asada, M., Satoh, M., Tanahashi, M., Yokota, T., Goto, S., 2022. Visualization of shallow subseafloor fluid migration in a shallow gas hydrate field using high-resolution acoustic mapping and ground-truthing and their implications on the formation process: a case study of the Sakata Knoll on the eastern margin of the Sea of Japan. *Mar. Geophys. Res.* 43, 1–18. <https://doi.org/10.1007/s11001-022-09495-9>
- Birth, G.A., 2003. A Scheme for Assessing Human Impacts on Coastal Aquatic Environments Using Sediments. Woodcoffe, C.D., Furness, R.A., Eds., Coastal GIS 2003, Wollongong University Papers in Centre for Maritime Policy, 14, Wollongong.
- Collier, R.W., 1985. Molybdenum in the Northeast Pacific Ocean. *Limnol. Oceanogr.* 30, 1351–1354.
- Gamo, T., Nakayama, N., Takahata, N., Sano, Y., Zhang, J., Yamazaki, E., Taniyasu, S., Yamashita, N., 2014. The Sea of Japan and Its Unique Chemistry Revealed by Time-Series Observations over the Last 30 Years. *Monogr. Environ. Earth Planets* 2, 1–22.
- Goto, S., Yamano, M., Morita, S., Kanamatsu, T., Hachikubo, A., Kataoka, S., Tanahashi, M., Matsumoto, R., 2017. Physical and thermal properties of mud-dominant sediment from the Joetsu Basin in the eastern margin of the Japan Sea. *Mar. Geophys. Res.* 38, 393–407.
- Hiruta, A., Wang, L.C., Ishizaki, O., Matsumoto, R., 2014. Last glacial emplacement of methane-derived authigenic carbonates in the Sea of Japan constrained by diatom assemblage, carbon-14, and carbonate content. *Mar. Pet. Geol.* 56, 51–62. <https://doi.org/10.1016/j.marpetgeo.2014.04.005>.
- Matsumoto, R., Ryu, B.J., Lee, S.R., Lin, S., Wu, S., Sain, K., Pecher, I., Riedel, M., 2011. Occurrence and exploration of gas hydrate in the marginal seas and continental margin of the Asia and Oceania region. *Mar. Pet. Geol.* 28, 1751–1767. <https://doi.org/10.1016/j.marpetgeo.2011.09.009>.
- Matsumoto, R., Tanahashi, M., Kakuwa, Y., Snyder, G., Ohkawa, S., Tomaru, H., Morita, S., 2017. Recovery of thick deposits of massive gas hydrates from gas chimney structures, eastern margin of Japan Sea Japan Sea shallow gas hydrate project. *Fire Ice* 17, 1–22. Available at: [https://www.netl.doe.gov/File Library/Research/Oil-Gas/methane hydrates/MHNews-2017-Jan.pdf](https://www.netl.doe.gov/File%20Library/Research/Oil-Gas/methane%20hydrates/MHNews-2017-Jan.pdf).
- McLennan, S.M., 2001. Relationships between the trace element composition of sedimentary rocks and upper continental crust. *Geochemistry, Geophys. Geosystems* 2, 2000GC000109.
- Miyajima, Y., Aoyagi, T., Yoshioka, H., Hori, T., A. Takahashi, H., Tanaka, M., Tsukasaki, A., Goto, S., Suzumura, M., 2024. Impact of Concurrent aerobic–anaerobic Methanotrophy on Methane Emission from Marine Sediments in Gas Hydrate Area. *Environ. Sci. & Technol.* 58, 4979–4988. <https://doi.org/10.1021/acs.est.3c09484>
- Miyajima, Y., Araoka, D., Yoshimura, T., Ota, Y., Suzuki, A., Yoshioka, H., Suzumura, M., Smrzka, D., Peckmann, J., Bohrmann, G., 2023. Lithium isotope systematics of methane-seep carbonates as an archive of fluid origins and flow rates. *Geochim. Cosmochim. Acta* 361, 152–170. <https://doi.org/10.1016/j.gca.2023.10.022>
- Ota, Y., Suzumura, M., Tsukasaki, A., Suzuki, A., Yamaoka, K., Asada, M., Satoh, M., 2022. Anaerobic oxidation of methane and trace-element geochemistry in microbial mat-covered sediments related to methane seepage, northeastern Japan Sea. *Chem. Geol.* 611, 121093. <https://doi.org/10.1016/j.chemgeo.2022.121093>

- Ota, Y., Iguchi, A., Nishijima, M., Mukai, R., Suzumura, M., Yoshioka, H., Suzuki, A., Tsukasaki, A., Aoyagi, T., Hori, T., 2024. Methane diffusion affects characteristics of benthic communities in and around microbial mat-covered sediments in the northeastern Japan sea. *Chemosphere* 349, 140964. <https://doi.org/10.1016/j.chemosphere.2023.140964>
- Senju, T., Aramaki, T., Tanaka, S. S., Zhang, J., Isoda, Y., Kumamoto, Y., Hibino, S., Nakano, T., 2013. Abyssal water mass exchange between the Japan and Yamato Basins in the Japan Sea. *J. Geophys. Res. Ocean.* 118, 4878–4888.
- Senju, T., Isoda, Y., Aramaki, T., Otosaka, S., Fujio, S., Yanagimoto, D., Suzuki, T., Kuma, K., Mori, K., 2005. Benthic front and the Yamato Basin Bottom Water in the Japan Sea. *J. Oceanogr.* 61, 1047–1058.
- Yanagawa, K., Kouduka, M., Nakamura, Y., Hachikubo, A., Tomaru, H., Suzuki, Y., 2014. Distinct microbial communities thriving in gas hydrate-associated sediments from the eastern Japan Sea. *J. Asian Earth Sci.* 90, 243–249. Available at: 10.1016/j.jseas.2013.10.019.